Int. J. Multiphase Flow Vol. 15, No. 2, pp. 135–154, 1989
Printed in Great Britain.

0301-9322/89 $3.00 + 0.00

ANALYSIS OF FUEL POLLUTANT MIGRATION IN WATER FLOW THROUGH POROUS MEDIA

A. PISTINER,[1] M. SHAPIRO[2]† and H. RUBIN[1]

[1]Faculty of Civil Engineering, CAMERI—Coastal and Marine Engineering Research Institute and
[2]Faculty of Mechanical Engineering, Technion—Israel Institute of Technology, Haifa 32000, Israel

(*Received* 18 *May* 1988; *in revised form* 4 *November* 1988)

Abstract—The penetration of a fuel pollutant from an external source into the groundwater is studied theoretically. The fuel migration in the aquifer is affected by viscous, capillary and gravitational forces. The contaminant is usually introduced into the main body of the aquifer due to seasonal oscillations of the groundwater level. Some portions of the fuel are trapped in the interstices of the porous medium. Other fuel portions are subjected to the flow as a continuous or a discontinuous phase. In this paper a one-dimensional model is developed describing the transport and accumulation of fuel in these two phases. By using power-law dependences of transport and kinetic properties of the fuel upon its saturation in the porous medium, several similarity solutions are obtained. The effect of fuel rupture and coalescence upon the migration of the bulk volume of the fuel spill is studied by employing a perturbation technique. As a result, the details of mass transfer between the continuous and the discontinuous fuel phases are provided.

Key Words: porous medium, two-phase flow, fuel rupture and coalescence, similarity solutions

INTRODUCTION

In the process of penetration into the aquifer some quantities of the fuel are trapped in the porous medium (Pfankuch 1984; Wilson & Conard 1984). Such trapped fuel quantities comprise the residual fuel saturation in the aquifer. Some other fuel quantities are subjected to flow in the aquifer. The fuel flowing as a continuous phase is eventually described by the classical laws of two-phase flow in porous media (Bear 1972). The process of fuel transfer between the continuous and the discontinuous phases is affected by various surface forces prevailing in the porous medium.

In the present study the process of fuel transfer between the two phases is modelled by an equation describing the kinetics of the interfacial fuel transfer (Spielman & Su 1977; Soo & Radke 1986). Such an equation refers to the phenomena of rupture and coalescence of fuel quantities occurring in the porous media. Physicochemical aspects of these phenomena can generally be described by thermodynamic laws (Morrow 1970).

Several theoretical models refer to the phenomenon of fuel droplet coalescence in porous media. Spielman & Goren (1972), Rosenfeld & Wasan (1974) and Spielman (1977) modelled the porous medium as a filter which purifies the water from the fuel droplets by causing their settling and coalescence, thereby creating a continuous fuel phase. Payatakes (1982) and Rosenfeld & Wasan (1974) accounted for the same mechanism while developing stochastic models of fuel rupture and coalescence. Spielman & Su (1977) carried out some laboratory studies demonstrating that the rate of growth of the discontinuous phase depends on the degree of saturation of the continuous and the discontinuous phases provided that the total fuel saturation is low.

Dependences of the capillary pressure and the hydraulic conductivity upon the degree of saturation can be determined experimentally, assuming that the equilibrium between the continuous and the discontinuous phases prevails. However, even if equilibrium conditions seem to take place in an experimental setup, frequently transfer processes between the continuous and the discontinuous fuel phases may continue (Morrow & Harris 1965). Usually a balance between different surface forces typical to the solid and fluid phases present in saturated porous media, prevails after a comparatively long time period.

†Bat-Sheva Fellow.

In experiments of imbibition the nonwetting phase moves slower than the wetting phase due to the tendency of the latter to by-pass the nonwetting phase. If the characteristic size of some pores is comparatively large and that of other pores comparatively small, then the phenomenon of "snap-off" may take place in which the fuel body is subject to rupture followed by trapping of some fuel quantities.

Another important phenomenon typical to flow of two fluid phases in porous media is called "Haines jumps" (Morrow 1970; Adler & Brenner 1988). This phenomenon is characterized by instantaneous changes of the capillary pressure caused by the process of build-up of fluid menisci in a porous medium. Morrow (1970) and Levine *et al.* (1980) claimed that Haines jumps should be attributed to abrupt changes in the characteristic diameter of the capillaries of the porous medium, leading to fuel transfer from metastable to completely stable conditions. Chen (1986) claimed that Haines jumps should be attributed to rupture or coalescence processes.

The objective of this study is to develop a quantitative model able to account for all the kinetic effects discussed in this section. We study the influence of the total fuel mass present in the porous medium on the fuel saturation profile and on the mass transfer between the continuous and the discontinuous fuel phases.

In general, the fuel saturation strongly depends on the capillary dispersion and the flow velocity. Due to this dependence the fuel transfer problem possesses a highly nonlinear character. This problem is treated here by utilizing the symmetry properties of the governing equations, thereby yielding several valuable similarity solutions.

In subsequent studies (Pistiner *et al.* 1989a, b) we investigate the influence of the pore size index of the porous medium and of the fuel viscosity on the advancement of the fuel saturation profile, the mass transfer and the kinetic processes occurring between the two fuel phases.

BASIC EQUATIONS

Consider an immiscible mixture of fuel and water transported along the x-axis in a homogeneous and isotropic porous medium. We will assume the gravity forces to be negligible and the fuel saturation of the continuous and the discontinuous phases to be sufficiently low. Under these conditions the respective specific discharges q_w and q_f of water and fuel are described by Darcy's law (Bear 1972):

$$q_w = -\frac{\kappa K_{rw}(S_f)}{\mu_w}\frac{\partial P_w}{\partial x} \qquad [1]$$

and

$$q_f = -\frac{\kappa K_{rf}(S_f)}{\mu_f}\frac{\partial P_f}{\partial x} \qquad [2]$$

with the relative permeabilities, K_{rw} and K_{rf} depending upon the fuel saturation, S_f (Bear 1972; Adler & Brenner 1988); and where κ is the permeability of the porous medium, μ_f and μ_w are the fuel and water viscosities, respectively and P_f and P_w are the fuel and water pressures, respectively. The fuel and water saturations, S_f and S_w, are related via the equation

$$S_f + S_w = 1, \qquad [3]$$

representing the fact that the porous medium is fully saturated by fuel and water. P_f and P_w are related via the capillary pressure P_c as follows:

$$P_c(S_f) = P_f - P_w, \qquad [4]$$

where

$$\frac{dP_c}{dS_f} > 0.$$

The conservation of mass for each fluid in a nonexpansive porous medium yields

$$\frac{\partial q_w}{\partial x} + \phi \frac{\partial S_w}{\partial t} = 0 \qquad [5]$$

and

$$\frac{\partial q_f}{\partial x} + \phi \frac{\partial S_f}{\partial t} = 0, \qquad [6]$$

where ϕ is the porosity of the porous medium. Combining [1]–[6] we obtain

$$\phi \frac{\partial S_f}{\partial t} = \frac{\partial}{\partial x}\left(\Psi \frac{\partial S_f}{\partial x}\right) - q \frac{\partial F}{\partial x}, \qquad [7]$$

where

$$q = q_w + q_f \qquad [8]$$

and the fractional flow curve F and the function Ψ are given by (Bear 1972)

$$F(S_f) = \left(\frac{1}{1 + \dfrac{K_{rw}\mu_f}{K_{rf}\mu_w}}\right) \qquad [9]$$

and

$$\Psi(S_f) = \frac{\kappa \dfrac{K_{rw} P_c'(S_f)}{\mu_w}}{\left(1 + \dfrac{K_{rw}\mu_f}{K_{rf}\mu_w}\right)}, \qquad [10]$$

where

$$P_c'(S_f) = \frac{dP_c(S_f)}{dS_f}.$$

The fuel saturation S_f can be expressed as follows (Morrow & Harris 1965; Spielman & Su 1977; Ramakrishnan & Wasan 1986):

$$S_f = S_{f_c} + S_{f_d}, \qquad [11]$$

where S_{f_c} is the degree of saturation of the continuous phase which moves according to the law of two-phase flow and S_{f_d} represents the degree of saturation of the stagnant discontinuous part of the fuel phase.

The parameters appearing in [9] and [10] may be assumed to depend only on S_{f_c} (Spielman & Su 1977). It is also assumed that the fuel transfer between the continuous and the discontinuous phases can be described by employing an isotherm represented by the following equation:

$$\frac{\partial S_{f_d}}{\partial t} = k_1 S_{f_c}^u - k_2 S_{f_d}^w. \qquad [12]$$

Here k_1 and k_2 are the kinetic coefficients of fuel transfer due to the rupture of the continuous phase and the coalescence of the discontinuous phase, respectively; u and w are positive constants which are determined from experimental data (Spielman & Su 1977). The kinetic equation of this type was used by Spielman & Su (1977) and by Payatakes (1982) to describe the fuel transport in porous media. Hougen & Marshal (1947) used [12] with $u = w = 1$. We will use this equation without the latter restriction so that to account for the nonlinear character of the adsorption–desorption processes.

Our goal is to investigate the effects of the rupture and the coalescence processes upon the fuel transport. It must be noted that the rupture and the coalescence processes are described by the characteristic times $1/k_1$ and $1/k_2$, respectively.

Fuel pollutants which are trapped in porous media may occupy no more than 50% of the pore volume (Wilson & Conrad 1984). In such cases it is possible to represent $F(S_{f_c})$ in [9] by a power-law relationship (Bear 1972; Ramakrishnan *et al.* 1988):

$$F(S_{f_c}) = F_0 S_{f_c}^n, \quad [13]$$

where the parameter n is a function of the viscosity ratio μ_f/μ_w, and F_0 is a scaling parameter. When $F(S_{f_c})$, given by [9], contains an inflection point, [13] is valid only when the fuel saturation is low. In addition, the derivative of the capillary pressure $P_c'(S_{f_c})$ and the relative permeability K_{rw} appearing in [10] obey the following relationship (Ramakrishnan *et al.* 1988; Yortsos & Fokas 1983):

$$P_c'(S_{f_c}) K_{rw}(S_{f_c}) = A_0 S_{f_c}^{-m}, \quad [14]$$

where

$$A_0 = \gamma_{fw} P_{c_0} K_{r_0}. \quad [15]$$

Here γ_{fw} is the fuel–water surface tension coefficient, P_{c_0} and K_{r_0} are positive constants which together with dimensionless coefficient m are determined by the pore-sized distribution of the porous medium. Equation [14] implies that the slope $dP_c/dS \to \infty$ as the saturation approaches zero. It should be noted that [14] assumes negligible changes in K_{rw} for low fuel saturations (Ramakrishnan *et al.* 1988).

Using [9] and [13]–[15] one can rewrite the function $\Psi(S_{f_c})$ given by [10] in the following form:

$$\Psi(S_{f_c}) = \frac{\kappa K_{r_0}}{\mu_w} F_0 P_{c_0} \gamma_{fw} S_{f_c}^{n-m}. \quad [16]$$

In the following, we will drop the subscript f when referring to the fuel saturations of the continuous and discontinuous phases, denoting them by S_c and S_d, respectively.

MATHEMATICAL FORMULATION

We define a characteristic convection length, L, and a characteristic convection time, T, as follows:

$$L = \kappa K_{r_0} P_{c_0} \quad [17]$$

and

$$T = \frac{L\Phi}{qF_0} \quad [18]$$

and introduce dimensionless spatial and temporal coordinates:

$$\hat{x} = \frac{xN_c}{L} \quad [19]$$

and

$$\hat{t} = \frac{tN_c}{T}, \quad [20]$$

where

$$N_c = \frac{\mu_w q}{\gamma_{fw}} \quad [21]$$

is the capillary number.

Expressions [7] and [12] rewritten in terms of dimensionless variables [19] and [20] adopt the following forms:

$$\frac{\partial S}{\partial \hat{t}} + \frac{\partial J_S}{\partial \hat{x}} = 0 \qquad [22]$$

and

$$\epsilon \frac{\partial S_d}{\partial \hat{t}} = S_c^u - \frac{1}{k} S_d^w, \qquad [23]$$

where $S = S_c + S_d$ is the total degree of fuel saturation, J_S is the flux of the fuel saturation and $k = k_1/k_2$ is the coefficient expressing the ratio between the rupture and the coalescence kinetic constants; k may be also interpreted as a ratio between the characteristic times of fuel coalescence $1/k_2$ and rupture $1/k_1$. The dimensionless parameter ϵ appearing in [23] is defined by

$$\epsilon = \frac{N_c}{k_1 T}. \qquad [24]$$

The fuel saturation flux J_S appearing in [22] possesses the following form:

$$J_S = S_c^n - S_c^{n-m} \frac{\partial S_c}{\partial \hat{x}}. \qquad [25]$$

Our objective is to solve [22] and [23] in the infinitely extended porous medium ($-\infty < \hat{x} < +\infty$). Accordingly, the saturation S_c and S_d are subjected to the following boundary conditions:

$$S_c(\hat{x}, \hat{t}) \to 0 \qquad |\hat{x}| \to \infty \qquad [26a]$$

and

$$S_d(\hat{x}, \hat{t}) \to 0 \qquad |\hat{x}| \to \infty. \qquad [26b]$$

The problem posed by [22], [23], [25] and [26a,b] must be solved for specified initial conditions imposed upon S_c and S_d. This problem, as posed above, describes the transport and accumulation of a given quantity of fuel initially (at time $t = 0$) distributed in the porous medium between the continuous and the discontinuous phases.

The total amount of fuel present in the porous medium is characterized by the characteristic fuel length L_M, given by

$$L_M = \int_{-\infty}^{+\infty} (S_c + S_d)\, dx. \qquad [27]$$

In the comparable three-dimensional case this quantity must be replaced by the characteristic fuel volume. In the present circumstances L_M may be interpreted as a characteristic volume per unit cross-section of the porous medium. This parameter represents a conserved property. The fact, that L_M is time independent may be verified by integration of [22] from $\hat{x} = -\infty$ to $\hat{x} = +\infty$ using boundary conditions [26a, b] imposed on S_c and S_d. We can thus define a dimensionless parameter

$$M_0 = \frac{N_c L_M}{L} = N_c L_M^* \equiv \int_{-\infty}^{+\infty} [S_c(\hat{x}, \hat{t}) + S_d(\hat{x}, \hat{t})]\, d\hat{x} \qquad [28]$$

which may be interpreted as a dimensionless fuel mass. Owing to the presence of the capillary number N_c and the convection length L, this quantity depends upon the capillary and the convective phenomena occurring in the porous medium.

We will be specifically interested in circumstances where the rupture and the coalescence processes are characterized by comparable characteristic times, each of them being much smaller than the characteristic convection time. These conditions may be described mathematically by the following relations:

$$k = O(1) \qquad [29]$$

and

$$\epsilon \ll 1. \qquad [30]$$

The case $\epsilon = 0$ describes the situation where a dynamic equilibrium exists between the fuel rupture and coalescence processes and the saturations S_c and S_d are related by the following equation:

$$S_c = \frac{1}{k^{1/u}} S_d^{w/u}. \tag{31}$$

The solution developed in the next section for small values of ϵ thus appears as a perturbation solution with respect to the equilibrium saturation distributions.

SOLUTION OF THE PROBLEM

The solution of the problem posed by [22], [23], [25] and [26a,b] is developed by the expansions of S_c, S_d and J_S in the power series of ϵ:

$$S_c(\hat{x}, \hat{t}, \epsilon) = S_{c_0}(\hat{x}, \hat{t}) + \epsilon S_{c_1}(\hat{x}, \hat{t}) + \cdots, \tag{32a}$$

$$S_d(\hat{x}, \hat{t}, \epsilon) = S_{d_0}(\hat{x}, \hat{t}) + \epsilon S_{d_1}(\hat{x}, \hat{t}) + \cdots \tag{32b}$$

and

$$J_S(\hat{x}, \hat{t}, \epsilon) = J^*_{S_0}(\hat{x}, \hat{t}) + \epsilon J^*_{S_1}(\hat{x}, \hat{t}) + \cdots, \tag{33}$$

where the zero-order functions S_{c_0}, S_{d_0} and $J^*_{S_0}$ refer to quantities which prevail in the equilibrium conditions. Introducing expansions [32a,b] and [33] into [22], [23], [25] and [26a,b] we obtain the following sequence of problems:

zero-order problem,

$$\frac{\partial (S_{c_0} + S_{d_0})}{\partial \hat{t}} + \frac{\partial J^*_{S_0}}{\partial \hat{x}} = 0, \tag{34}$$

$$J^*_{S_0} = S^n_{c_0} - S^{n-m}_{c_0} \frac{\partial S_{c_0}}{\partial \hat{x}}, \tag{35}$$

$$S^u_{c_0} = \frac{1}{k} S^w_{d_0}, \tag{36}$$

$$S_{c_0}(\hat{x}, \hat{t}) \to 0 \qquad |\hat{x}| \to \infty \tag{37a}$$

$$S_{d_0}(\hat{x}, \hat{t}) \to 0 \qquad |\hat{x}| \to \infty; \tag{37b}$$

and

first-order problem,

$$\frac{\partial (S_{c_1} + S_{d_1})}{\partial \hat{t}} + \frac{\partial J^*_{S_1}}{\partial \hat{x}} = 0, \tag{38}$$

$$J^*_{S_1} = (n-m) S_{c_1} S^{n-m-1}_{c_0} \frac{\partial S_{c_0}}{\partial \hat{x}} - S^{n-m}_{c_0} \frac{\partial S_{c_1}}{\partial \hat{x}} + n S_{c_1} S^{n-1}_{c_0}, \tag{39}$$

$$\frac{\partial S_{d_0}}{\partial \hat{t}} = u S^{u-1}_{c_0} S_{c_1} - \frac{w}{k} S_{d_0} S_{d_1}, \tag{40}$$

$$S_{c_1}(\hat{x}, \hat{t}) \to 0 \qquad |\hat{x}| \to \infty \tag{41a}$$

$$S_{d_1}(\hat{x}, \hat{t}) \to 0 \qquad |\hat{x}| \to \infty. \tag{41b}$$

We will further look for simultaneously existing similarity solutions of the problems posed by [34]–[37a,b] and [38]–[41a,b]. These solutions implicitly assume that the saturation functions S_{c_0}, S_{d_0}, S_{c_1} and S_{d_1} achieve certain asymptotic forms in which they are described by a single variable ξ, given by (Barenblatt 1979)

$$\xi = \hat{x}\hat{t}^{-a}, \tag{42}$$

where a is a constant to be determined below. The solutions for the zero- and first-order saturation functions are sought in the following forms (Ramakrishnan *et al.* 1988):

$$S_{c_0} = f_{c_0}\hat{t}^{b}, \quad S_{d_0} = f_{d_0}\hat{t}^{c}, \quad S_{c_1} = f_{c_1}\hat{t}^{d}, \quad S_{d_1} = f_{d_1}\hat{t}^{l}, \tag{43a–d}$$

where the functions f_{c_0}, f_{d_0}, f_{c_1} and f_{d_1} depend upon ξ only and b, c, d and l are constant values. The existence of the similarity solution implies that

$$u = w, \quad b = c, \quad d = l. \tag{44a–c}$$

Introducing the trial solution [43a–d] into condition [28] we obtain

$$M_0 = \hat{t}^{a+b}\int_{-\infty}^{+\infty}(f_{c_0}+f_{d_0})\,\mathrm{d}\xi + \epsilon\hat{t}^{a+d}\int_{-\infty}^{+\infty}(f_{c_1}+f_{d_1})\,\mathrm{d}\xi. \tag{45}$$

The requirement of mass conservation yields the following additional conditions:

$$a + b = 0, \quad m = 2 \tag{46a,b}$$

and

$$\int_{-\infty}^{+\infty}(f_{c_1}+f_{d_1})\,\mathrm{d}\xi = 0. \tag{47}$$

Equations [44a–c] and [46a,b] combine to yield

$$a = \frac{1}{n}, \tag{48a}$$

$$b = c = -\frac{1}{n}, \tag{48b}$$

and

$$d = l = \frac{u-n-2}{n}. \tag{48c}$$

It thus follows that transformations [42] and [43a–d] adopt the following forms:

$$\xi = \hat{x}t^{-1/n}$$

and

$$S_{c_0} = f_{c_0}\hat{t}^{-1/n}, \quad S_{d_0} = f_{d_0}\hat{t}^{-1/n}, \quad S_{c_1} = f_{c_1}\hat{t}^{(u-n-2)/n}, \quad S_{d_1} = f_{d_1}\hat{t}^{(u-n-2)/n}.$$

Introduction of S_{c_0} and S_{d_0}, given by [43a,b], into [34] and [35] for the zero-order problem after some simplifications yields the following ordinary differential equations:

$$\left(f'_{c_0}f_{c_0}^{n-2} - f_{c_0}^{n} + \frac{1+k^{1/u}}{n}\xi f_{c_0}\right)' = 0 \tag{49}$$

and

$$f_{d_0} = k^{1/u}f_{c_0}. \tag{50}$$

Boundary conditions for the zero-order functions f_{c_0} and f_{d_0} are obtained from [43a,b] and [37a,b]:

$$f_{c_0}, f_{d_0} \to 0 \qquad |\xi| \to \infty. \tag{51a,b}$$

The first-order problem [38]–[41a,b] in terms of the new variables given by [43a–d] adopts the following form:

$$\left[-2f_{c_0}^{n-1}f_{c_1}-(n-2)\frac{1+k^{1/u}}{n}f_{c_1}\xi+f_{c_0}^{n-2}f'_{c_1}+\frac{\xi}{n}(f_{c_1}+f_{d_1})\right]'=\frac{u-n-1}{n}(f_{c_1}+f_{d_1}), \qquad [52]$$

$$f_{d_1}=k^{1/u}f_{c_1}+\frac{k^{2/u}}{un}\left(f_{c_0}^{2-u}+\xi f_{c_0}^{3-u}-\xi^2\frac{1+k^{1/u}}{n}f_{c_0}^{4-u-n}\right) \qquad [53]$$

$$f_{c_1}, f_{d_1}\to 0 \qquad |\xi|\to\infty. \qquad [54a,b]$$

The zero-order problem [49]–[51a, b] may be simplified. Indeed, integration of [49] yields

$$f_{c_0}^{n-2}f'_{c_0}+\frac{1+k^{1/u}}{n}\xi f_{c_0}-f_{c_0}^{n}=C_1, \qquad [55]$$

where C_1 is an integration constant. We will assume that f_{c_0} and f_{d_0} decay sufficiently fast so that all terms appearing on the l.h.s. of [55] tend to zero when $|\xi|\to\infty$. Therefore we obtain $C_1=0$. As a result, [55] reduces to

$$f'_{c_0}=f_{c_0}^{2}-\frac{1+k^{1/u}}{n}\xi f_{c_0}^{3-n}. \qquad [56]$$

Introduction of [43a–d] into [32a,b] gives

$$S_c(\hat{x},\hat{t},\epsilon)=\hat{t}^{-1/n}(f_{c_0}+\epsilon\hat{t}^{(u-n-1)/n}f_{c_1})+O(\epsilon^2) \qquad [57a]$$

and

$$S_d(\hat{x},\hat{t},\epsilon)=\hat{t}^{-1/n}(f_{d_0}+\epsilon\hat{t}^{(u-n-1)/n}f_{d_1})+O(\epsilon^2). \qquad [57b]$$

These equations indicate that

$$\frac{u-n-1}{n}<0, \qquad [58]$$

which is dictated by the requirement of the smallness of the second terms on the r.h.s. of [57a,b] for $\hat{t}\to\infty$.

ANALYSIS OF THE LIMITATIONS IMPOSED ON n

Expression [56] together with the boundary conditions [51a,b] yield the following asymptotic behavior:

$$f'_{c_0}\sim-\frac{1+k^{1/u}}{n}\xi f_{c_0}^{3-n} \qquad |\xi|\to\infty, \qquad [59]$$

which is valid at least for $n\geqslant 1$. Integration of [59] gives

$$f_{c_0}\sim\frac{1}{\left[(2-n)\dfrac{1+k^{1/u}}{2n}\xi^2+C_2\right]^{1/(2-n)}} \qquad |\xi|\to\infty. \qquad [60]$$

The condition of positiveness of the denominator in [60] yields the following limitation imposed upon n:

$$n<2. \qquad [61]$$

Straightforward analysis of [59] shows that the case $n=2$ also yields the rapidly decaying asymptotic behavior of f_{c_0} as $|\xi|\to\infty$. We will further consider the following range of n:

$$1\leqslant n\leqslant 2. \qquad [62]$$

The case $n>2$ leads to the formation of the fuel–water free boundary and is treated in a subsequent paper (Pistiner *et al.* 1989a).

ANALYSIS OF THE GLOBAL FUEL MIGRATION

The similarity solution developed above describes the global migration of a fuel slug initially introduced in the porous medium. Here we utilize the transformation [48a] to evaluate the mean propagation velocity of the fuel slug, defined by

$$V = \frac{\mathrm{d}\bar{\hat{x}}}{\mathrm{d}\hat{t}}, \tag{63}$$

where $\bar{\hat{x}}$ is the mean fuel displacement:

$$\bar{\hat{x}} = \frac{1}{M_0}\int_{-\infty}^{+\infty} \hat{x}[S_c(\hat{x}, \hat{t}) + S_d(\hat{x}, \hat{t})]\,\mathrm{d}\hat{x}. \tag{64}$$

The rate of fuel spread is described by the mean square displacement:

$$\overline{(\hat{x} - \bar{\hat{x}})^2} = \frac{1}{M_0}\int_{-\infty}^{+\infty} (\hat{x} - \bar{\hat{x}})^2[S_c(\hat{x}, \hat{t}) + S_d(\hat{x}, \hat{t})]\,\mathrm{d}\hat{x}. \tag{65}$$

Introducing [43a] together with [48a,b] into [63], [64] and [65] we obtain (neglecting the first-order terms):

$$V = \frac{1}{nM_0}\hat{t}^{(1-n)/n}\int_{-\infty}^{+\infty} (1 + k^{1/u})\xi f_{c_0}\,\mathrm{d}\xi \tag{66}$$

and

$$\overline{(\hat{x} - \bar{\hat{x}})^2} = \frac{1}{nM_0}\hat{t}^{2/n}\int_{-\infty}^{+\infty} (1 + k^{1/u}) f_{c_0}(\xi - \bar{\hat{x}})^2\,\mathrm{d}\xi. \tag{67}$$

The integrals on the r.h.s.s of [66] and [67] are numbers that can be evaluated for each set of n, k and u. Therefore [66] and [67] exhibit time dependences of the mean velocity and the mean square displacement as follows:

$$V \sim \hat{t}^{(1-n)/n}$$

and

$$\overline{(\hat{x} - \bar{\hat{x}})^2} \sim \hat{t}^{2/n}.$$

It is interesting to note that for $n = 1$ the fuel profile propagates with a constant velocity. In the considered range $1 \leqslant n \leqslant 2$ the fuel velocity decays with time. When $n = 2$ the rate of fuel dispersion is constant. This conclusion may be also drawn directly from [35].

ALTERNATIVE INTERPRETATION OF THE ZERO-ORDER SOLUTION

Equations [34] and [35] with $m = 2$ (which is a necessary condition for the mass conservation) combined with [42], [43a,b], [48a,b] and [56] may be rewritten in the following form:

$$\frac{\partial S_{c_0}}{\partial \hat{t}} + \frac{\partial J_{S_0}}{\partial \hat{x}} = 0, \tag{68a}$$

where

$$J_{S_0} = \frac{S_{c_0}\hat{x}}{n\hat{t}} = \frac{J^*_{S_0}}{(1 + k^{1/u})}. \tag{68b}$$

is the reduced fuel saturation flux.

This is the kinematic wave equation in which the wave velocity is $\hat{x}/(n\hat{t})$. It may be seen that this $\hat{x}$ and $\hat{t}$ dependence of the wave velocity does not lead to shock formation (Tondeur 1987). An elementary analysis of [68a,b] yields the following characteristic solution:

$$\xi = \hat{x}\hat{t}^{-1/n} \tag{69a}$$

and

$$S_{c_0} = f_{c_0}(\xi)\hat{t}^{-1/n}, \tag{69b}$$

which explicitly reproduces the similarity variables in [42] and [43a].

One can also rewrite [68a] in the following form:

$$\frac{\partial S_{c_0}}{\partial \hat{t}} + W_c \frac{\partial S_{c_0}}{\partial \hat{x}} = 0, \tag{70a}$$

where

$$W_c = \left[\frac{\partial J_{S_0}}{\partial S_{c_0}}\right]_t = U_S + S_{c_0}\left[\frac{\partial U_S}{\partial S_{c_0}}\right]_t \tag{70b}$$

and

$$U_S = \frac{\hat{x}}{n\hat{t}}.$$

This form will be useful in analyzing the effect of the characteristic fuel mass M_0 upon the saturation profile.

ANALYTICAL SOLUTIONS OF THE ZERO-ORDER PROBLEM

Equation [56] for $n = 2$ is a Riccati-type equation possessing the following solution:

$$f_{c_0}(\xi) = \frac{\exp\left(-\dfrac{1+k^{1/u}}{4}\xi^2\right)}{f_{c_0}^{-1}(0) - \sqrt{\dfrac{\pi}{1+k^{1/u}}}\,\mathrm{erf}\left(\dfrac{\sqrt{1+k^{1/u}}}{2}\xi\right)}. \tag{71a}$$

The value $f_{c_0}(0)$ is related to the dimensionless total fuel mass M_0 as follows:

$$f_{c_0}(0) = \sqrt{\frac{1+k^{1/u}}{\pi}}\tanh\left(\frac{M_0}{2}\right) \tag{72}$$

with the following limitation imposed upon $f_{c_0}(0)$:

$$f_{c_0}(0) < \sqrt{\frac{1+k^{1/u}}{\pi}}.$$

Substituting $f_{c_0}(0)$, given by [72], into [71a] one can rewrite the solution for $f_{c_0}(\xi)$ in the following form:

$$f_{c_0}(\xi) = \sqrt{\frac{1+k^{1/u}}{\pi}}\,G(\zeta), \tag{71b}$$

where G is a function of the variable $\zeta = \xi(\sqrt{1+k^{1/u}}/2)$. Since k does not appear explicitly in $G(\zeta)$, [71b] is helpful in revealing the influence of this parameter on the saturation function $f_{c_0}(\xi)$. For a given M_0, an increase in k decreases the fuel mass present in the continuous phase and leads to a sharper saturation profile with the maximum value of the saturation growing proportionally to $\sqrt{1+k^{1/u}}$.

For $n = 1$, [56] possesses the following analytical solution:

$$f_{c_0}(\xi) = \frac{1}{f_{c_0}^{-1}(0) - \xi + \dfrac{1 + k^{1/u}}{2}\xi^2}, \qquad [73]$$

where $f_{c_0}(0)$ is related to the dimensionless mass M_0 via the relationship

$$f_{c_0}(0) = \frac{2(1 + k^{1/u})M_0^2}{M_0^2 + 4\pi^2(1 + k^{1/u})^2}. \qquad [74]$$

It is clear that $f_{c_0}(0) < 2(1 + k^{1/u})$.

DISCUSSION OF THE ZERO-ORDER RESULTS

Figures 1–4 depict the propagation of the saturation profiles for the cases $n = 1$ and $n = 2$. Figures 2 and 4 describe the case where $L_M \gg L$, namely an infinite dimensionless mass M_0. Figures 2 and 4 describe the propagation of the saturation profiles in the water flow direction. On the other hand, figures 1 and 3 describe circumstances where the fuel moves against the flow of water. Figures 1–4 clearly exhibit the phenomena of fuel imbibition and drainage in the porous medium. However, at a given location within the porous medium these phenomena may be better observed in figures 5 and 6, depicting the relationship between the fuel flux and the saturation for several given time values (see [68a,b]). Each of the curves shown in figures 5 and 6 may be characterized by the following regions, specified in figure 5:

(1) region AB describing fuel drainage against the water flow direction;
(2) region BC describing fuel imbibition in the water flow direction;
(3) region CD describing fuel imbibition against the water flow direction;
(4) region DA describing the fuel drainage in the water flow direction.

Comparing the data shown in figure 5 obtained for finite M_0 with the data in figure 6 obtained for infinite M_0 we can see that for increasing M_0, the fuel convective transport is enhanced with respect to the transport due to fuel dispersion against the water flow direction.

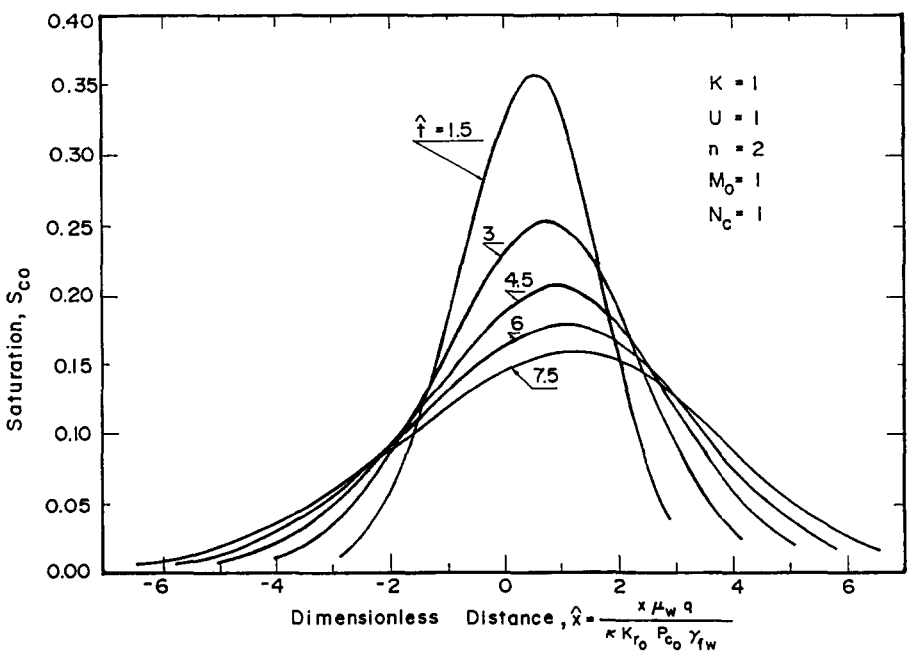

Figure 1. Propagation of the saturation profile for low M_0 (zero-order solution, $m = 2$).

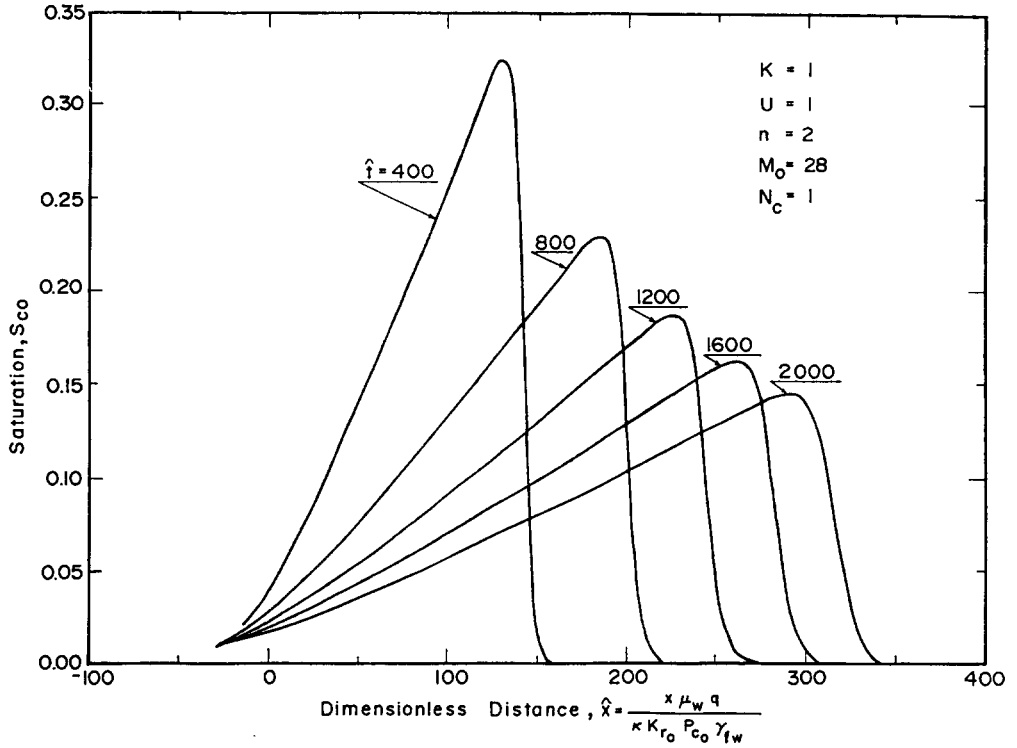

Figure 2. Propagation of the saturation profile for high M_0 (zero-order solution, $m = 2$).

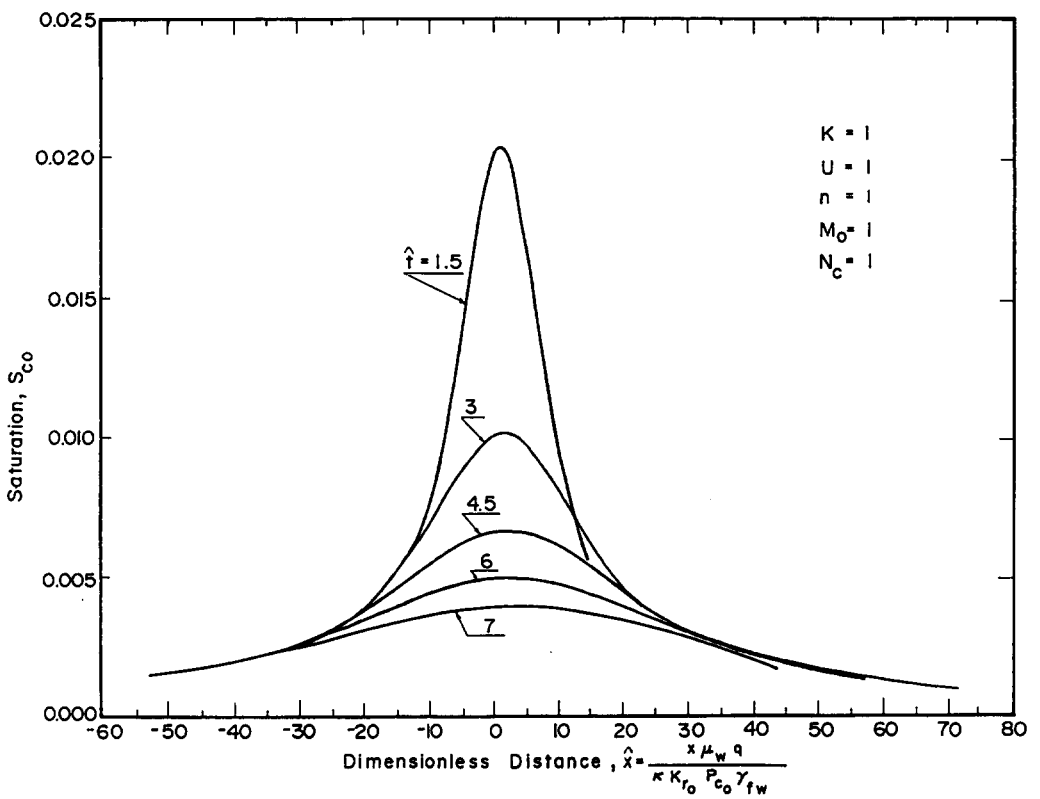

Figure 3. Propagation of the saturation profile for low M_0 (zero-order solution, $m = 2$).

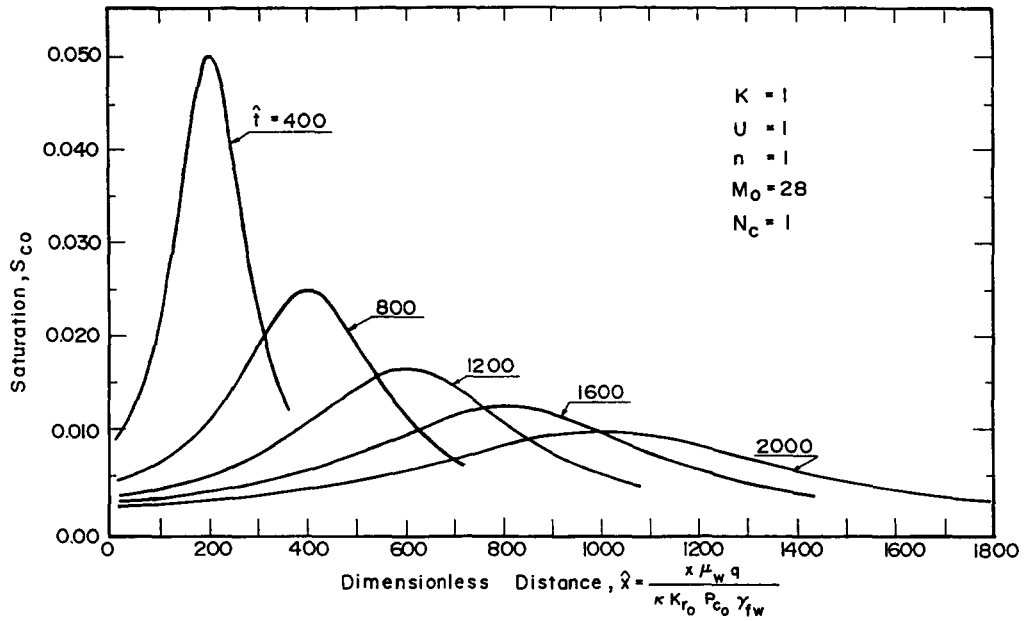

Figure 4. Propagation of the saturation profile for high M_0 (zero-order solution, $m = 2$).

The value of the group velocity W_c given by [70b] is represented by the slope of the curves appearing in figures 5 and 6 (see [70a]). We will now analyze the behavior of W_c for very large M_0 (see figure 6). Towards this goal use [56] to express the location, ξ_m, of the maximum value of the function $f_{c_0}(\xi)$ in the following form:

$$\xi_m = \frac{n f_{c_0}^{n-1}(\xi_m)}{1 + k^{1/u}}. \qquad [75a]$$

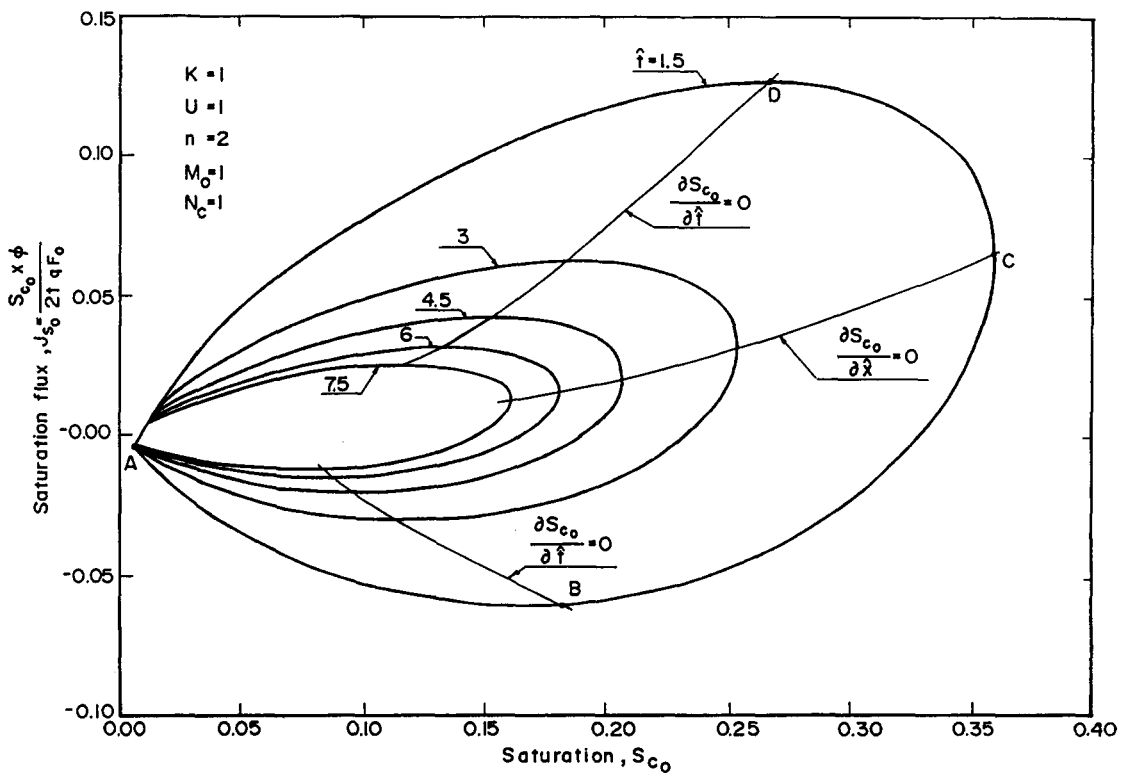

Figure 5. Fuel flux vs fuel saturation for several values of time (zero-order solution, low M_0).

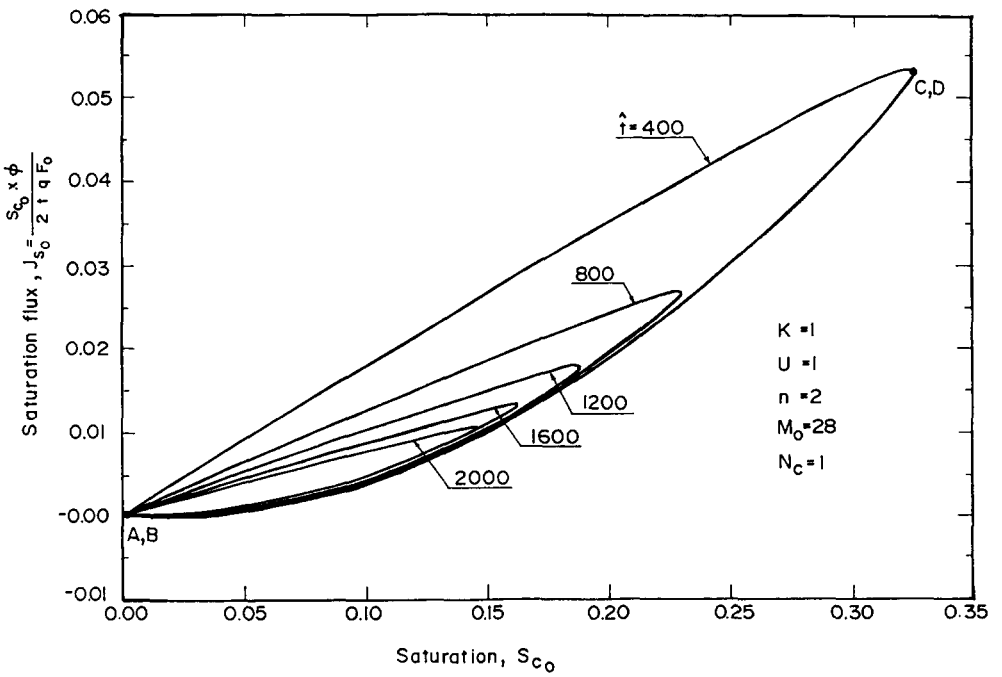

Figure 6. Fuel flux vs fuel saturation for several values of time (zero-order solution, high M_0).

We consider the following cases.

$n = 2$

The information for this case is shown in figure 6. For $n = 2$ [75a] reduces to

$$\xi_m = \frac{2 f_{c_0}(\xi_m)}{1 + k^{1/u}}. \tag{75b}$$

Analysis of [71a] and [72] shows that the maximum value of $f_{c_0} \to \infty$ for increasing values of the dimensionless mass M_0. Equation [75b] shows that the location of that maximum moves towards larger values of ξ when $M_0 \to \infty$. It can be shown that

$$\xi_{m_*} < 2\sqrt{\frac{M_0}{1 + k^{1/u}}}. \tag{76a}$$

The value appearing on the r.h.s. of [76a] may be used as a satisfactory estimate for ξ_{m_*} for large M_0.

The descending branch of the zero-order similarity solution is characterized by a sharp transition from a very large to a small (almost zero) value of f_{c_0}. The approximate location ξ_{m_*} of this sharp transition can be found numerically for every M_0 via [71a]. Accordingly, figure 2 shows that with an increasing M_0 the region of fuel imbibition becomes large (cf. figure 1, obtained for $M_0 = 1$) while drainage occurs in a very narrow range of $\hat{x}$, immediately reducing S_{c_0} to zero. This sharp stepwise behavior of S_{c_0} reflects a comparable property of the function $f_{c_0}(\xi)$ discussed above.

Fuel saturation flux at the point $\xi = \xi_{m_*}$ can be obtained by introduction of [69b] and [75b] into [68b], thus resulting in

$$J_{S_0}(\hat{x}_{m_*}, \hat{t}) = \frac{S_{c_0}^2(\hat{x}_{m_*}, \hat{t})}{1 + k^{1/u}}, \tag{76b}$$

where

$$\hat{x}_{m_*} = \xi_{m_*} \hat{t}^{1/2}$$

and the group velocity at the ascending branches in figure 2 adopts the following form:

$$W_c = \left[\frac{\partial J_{S_0}}{\partial S_{c_0}}\right]_{\hat{t}} = \frac{2 S_{c_0}(\hat{x}_{m_*}, \hat{t})}{1 + k^{1/u}}. \tag{76c}$$

Equation [76b] describes the lowermost parts of curves common to all values of the time $\hat{t}$ represented in figure 6. The time-independent behavior of these ascending branches stems from the assumed time-independent character of the specific discharge in [8]. The velocities given by [70b] of the descending branches of the saturation profiles depicted in figure 2 may be shown to exhibit the following behavior:

$$W_c|_{\xi_{m_*}+0} = \left[\frac{\xi_{m_*}}{2} - \frac{1}{(1+k^{1/u})\xi_{m_*}}\right]\frac{1}{\sqrt{\hat{t}}} \qquad [77]$$

and are described by the upper parts (almost straight lines) of the curves plotted in figure 6. From [77] it can be seen that the velocity of the descending branch decays with time.

n = 1

In this case we obtain from [75a]:

$$\xi_m = \frac{1}{1+k^{1/u}}. \qquad [78]$$

The position of the maximum saturation is independent of the fuel characteristic mass M_0. By using the same procedure as in the previous case we obtain

$$W_c \to \frac{1}{1+k^{1/u}}, \qquad \text{as } M_0 \to \infty.$$

In these circumstances the fuel saturation profile moves with a constant velocity along the flow direction, as shown in figure 4.

In general, an increase in n from $n = 1$ to $n = 2$ leads to an enhancement of the convective fuel transport with respect to the dispersive transport.

THE FIRST-ORDER SOLUTION

It may be seen from [23] that the kinetic processes are governed by the dimensionless time

$$\tilde{t} = \frac{\hat{t}}{\epsilon} = \frac{tk_1}{N_c}.$$

This means that the long-time limit $\hat{t} \to \infty$ is equivalent to the case of a very fast kinetic process described by $k_1 \to \infty$ (N_c is a constant number in this problem). Referring to [24] we can see that the latter condition may be interpreted as $\epsilon \to 0$. That is, for a given rate of convection–diffusion processes the fuel exchange between the continuous and the discontinuous phases occurs very fast, so that one witnesses an equilibrium prevailing between these phases. The observed equivalence between the two cases $\hat{t} \to \infty$ and $\epsilon \to 0$ is further used to formulate additional conditions imposed upon the first-order saturation functions S_{d_1} and S_{c_1}. Indeed, observing [22], [32a,b] and [33] one can state that

$$S_{c_1}(\hat{x}, \hat{t}) + S_{d_1}(\hat{x}, \hat{t}) = 0 \qquad \hat{t} \to \infty \qquad [79a]$$

$$J^*_{S_1}(\hat{x}, \hat{t}) = 0 \qquad \hat{t} \to \infty. \qquad [79b]$$

This means that for asymptotically long times ($\xi \to 0$) fuel saturation is represented by the zero-order functions only. In order to reformulate these boundary conditions in the self-similar form we use [42] and [48a] which immediately yield

$$f_{c_1}(0) + f_{d_1}(0) = 0 \qquad [80a]$$

and

$$-2f_{c_1}(0)f_{c_0}^{n-1}(0) + f'_{c_1}(0)f_{c_0}^{n-2}(0) = 0. \qquad [80b]$$

The solution of the problem posed by [22]–[26] in the physical plane $(\hat{x}, \hat{t})$ obviously depends upon the specified initial condition. However the similarity solutions for S_{c_0}, S_{d_0}, S_{c_1} and S_{d_1} in the form [48a] do not generally reproduce the chosen initial fuel saturation profiles. However, the zero-order functions exhibit the following short-time dependences:

$$S_{c_0}, S_{d_0} \to \delta(\hat{x}), \qquad \text{as } \hat{t} \to 0,$$

where $\delta(\hat{x})$ is the Dirac δ-function.

It should be noted that the existence of the self-similar solution reflects the property of the function $\hat{S}(\hat{x}, \hat{t})$, that it "forgets" the initial saturation profile. Eventually it tends to the above developed similarity solution for asymptotically long times. Both solutions in the $\hat{x} - \hat{t}$ and the self-similar domains are characterized by the same value of the total amount of fuel or the characteristic dimensionless fuel length L_M^*, given by [28].

Figures 7 and 8 show the first-order saturation solutions, f_{c_1} and f_{d_1}, appearing in [52]–[54a,b]. In general these functions represent the deviation of the saturations S_c and S_d from their equilibrium values S_{c_0} and S_{d_0} (see [57a,b]). Figures 7 and 8 indicate that for asymptotically long times ($\xi \to 0$) $S_{d_1} > 0$, $S_{c_1} < 0$. Hence the continuous phase contains less fuel than it does in the equilibrium case ($\epsilon = 0$).

Figures 9 and 10 exhibit the temporal evolution of the fuel saturation in various points $\hat{x}$ with and without kinetically induced distortion for low M_0. The saturation fluctuations observed in figure 10 may be identified with the above-described "Haines jumps" which are mentioned in the introduction of this article. Our results reveal that this phenomenon stems from the movement of fuel menisci due to rupture and coalescence of the fuel phase, prior to reaching the equilibrium state. This confirms the earlier observation of Chen (1986).

We define a ratio K_L between the typical fuel lengths of the discontinuous and the continuous phases as follows:

$$K_L = \frac{k^{1/u}\int_{-\infty}^{+\infty} f_{c_0}\,d\xi + \epsilon \hat{t}^{(u-n-1)/n}\int_{-\infty}^{+\infty} f_{d_1}\,d\xi}{\int_{-\infty}^{+\infty} f_{c_0}\,d\xi + \epsilon \hat{t}^{(u-n-1)/n}\int_{-\infty}^{+\infty} f_{c_1}\,d\xi} = \frac{L_{\text{disc.}}}{L_{\text{con.}}}, \qquad [81]$$

which is plotted in figure 11 vs time. For long times the ratio $K_L(\epsilon, \hat{t})$ tends to the value $k^{-1/u}$, thereby describing the equilibrium situation. However for earlier times, before the equilibrium is achieved, more fuel is present in the discontinuous phase than in the continuous phase thus resulting in larger values of K_L as indicated in figure 11.

Figure 12 indicates that for low M_0 the function $f_{c_0}(\xi)$ tends to be symmetric, namely $f_{c_0}(-\xi) = f_{c_0}(+\xi)$. It means that the capillary dispersion is more intensive than fuel convection, whereas the latter generally causes an asymmetry in the fuel distribution. As a result, we observe

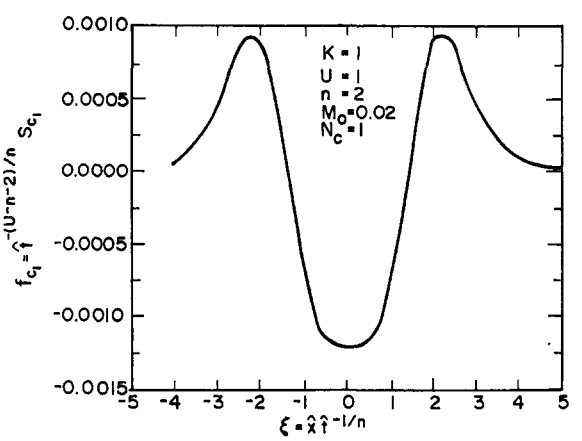

Figure 7. First-order similarity solution profile (f_{c_1}).

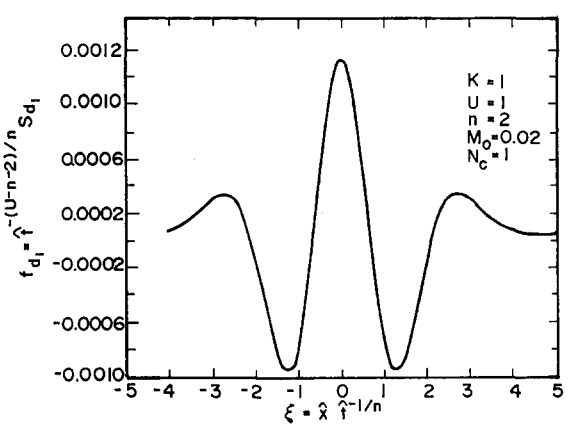

Figure 8. First-order similarity solution profile (f_{d_1}).

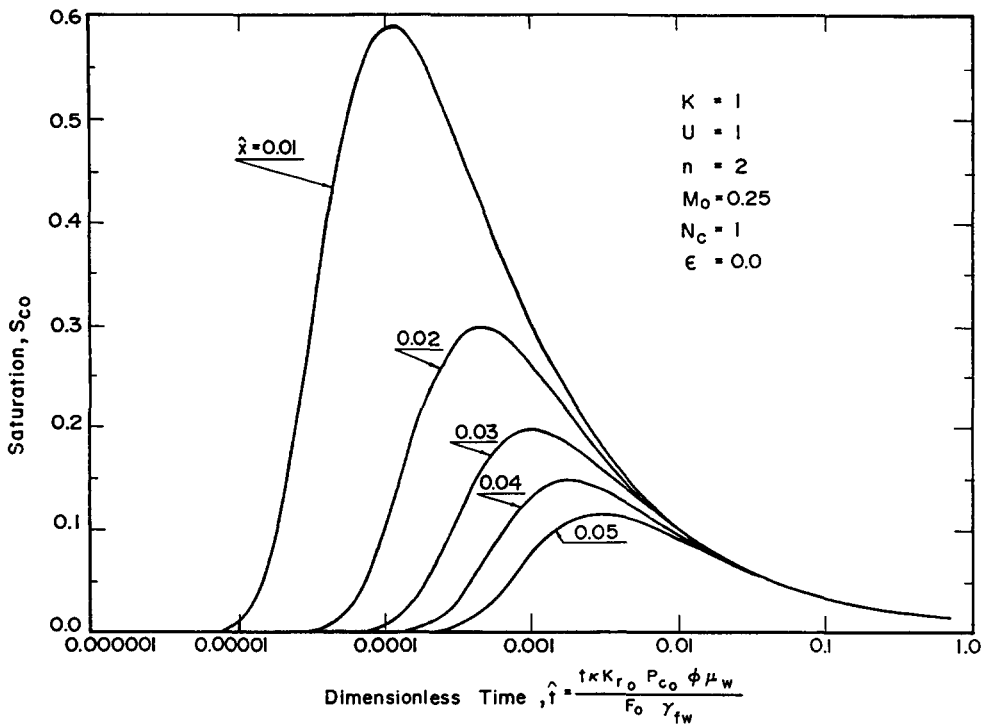

Figure 9. Temporal evolution of the equilibrium fuel saturation at various points $\hat{x}$.

more fuel drainage rather than imbibition, as indicated by figures 9 and 10. As evidenced by [53], for long times ($\xi \to 0$) more fuel is present in the discontinuous rather than in the continuous phase. This fact, of course, is true only for times preceding the equilibrium state, e.g., for finite $\hat{t}$, since for the equilibrium state the distribution of fuel between the phases is entirely governed by the kinetic constant k.

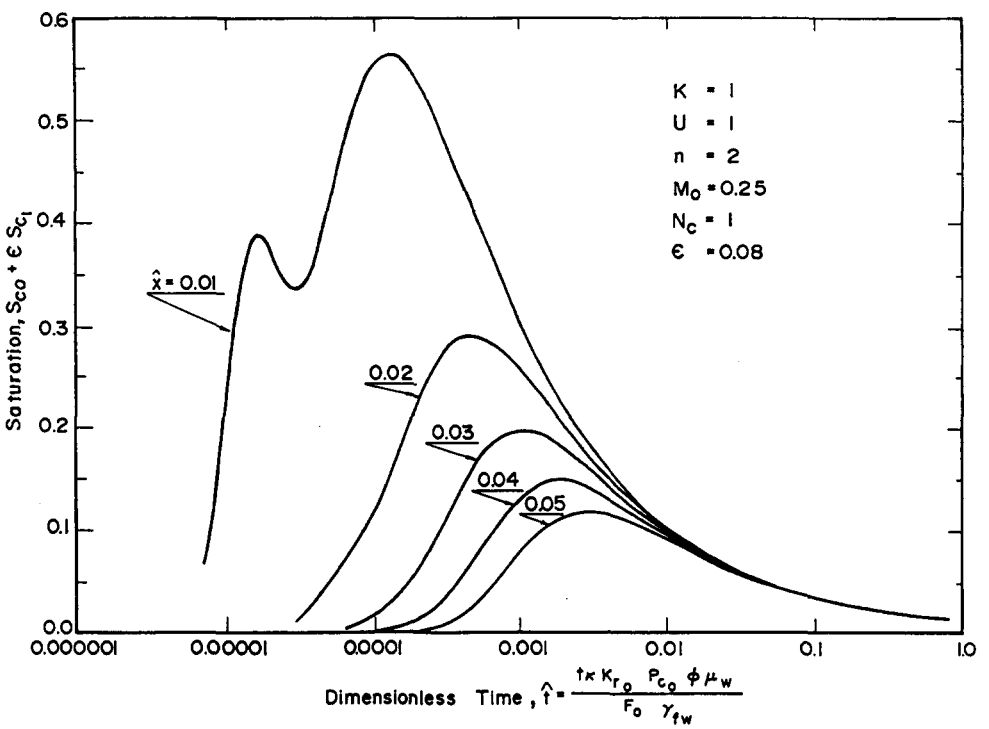

Figure 10. Temporal evolution of fuel saturation at various points $\hat{x}$ in the absence of equilibrium.

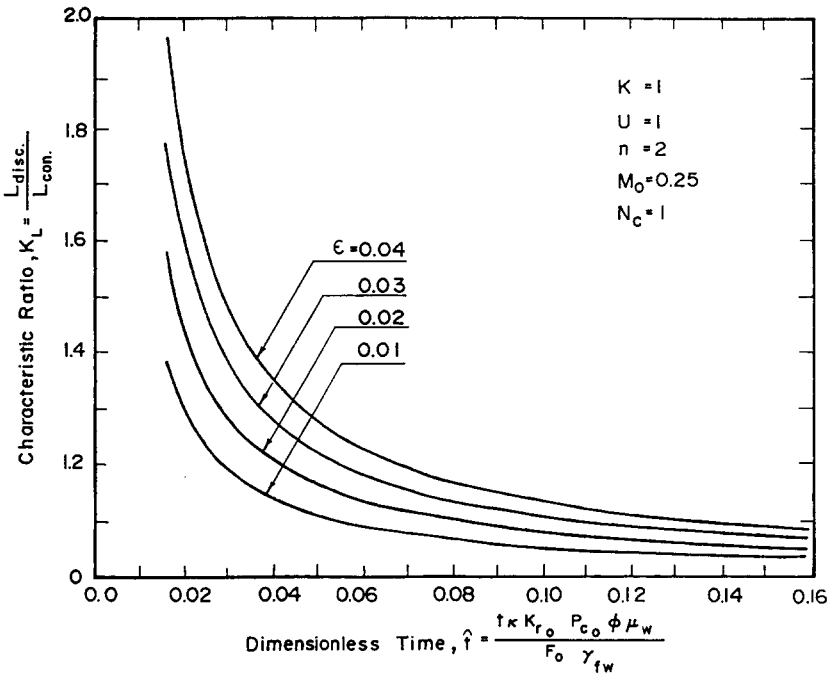

Figure 11. Characteristic ratio of typical lengths of the discontinuous and the continuous fuel phases vs time.

We finally observe that the imbibed fuel in the continuous phase tends to be ruptured and left behind in the discontinuous phase.

SUMMARY AND CONCLUSIONS

The migration of fuel pollutant in porous media is modelled by means of the equations describing mass transport and kinetic processes occurring in the moving (continuous) and the residual (discontinuous) phases.

In this study we referred to the problem of fuel pollutant migration through a porous medium, where it was assumed that continuous and discontinuous fuel phases are subjected to a dynamic equilibrium existing between them (in the zero-order problem).

The distribution of fuel between the continuous and the discontinuous phases is affected by the partition coefficient k, governing the equilibrium condition (cf. [13]). Our results provide a quantitative measure for the fuel saturation in both phases, which may be obtained utilizing the experimentally determined (Land 1968, 1971) coefficient k.

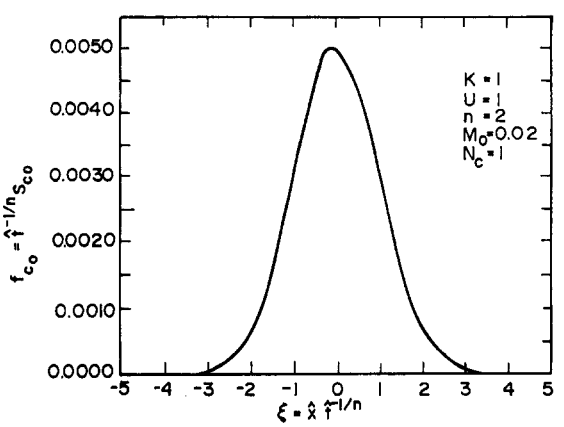

Figure 12. Zero-order similarity solution profile (f_{c_0}) for low M_0.

In contrast with existing models (e.g. Bear 1972; Ramakrishnan *et al.* 1988) assuming the discontinuous (residual) fuel saturation to be constant and uniform, our treatment described the accumulation of the residual phase and its migration in the porous medium. This migration is modelled as occurring due to the fuel exchange between the residual and the continuous flowing fuel phase.

The influence of the total amount of fuel M_0 present in the porous medium on the rate of kinetic processes of fuel rupture and coalescence was investigated. It was found that for low values of M_0 small deviations from the dynamic equilibrium lead to the "Haines jumps" phenomenon.

It is found that for low values of the dimensionless characteristic fuel length scale, L_M^*, the kinetic processes are slow compared to the convective–dispersive fuel transport. On the contrary, for high values of L_M^* the kinetic processes occur much faster than the fuel transport, so that an equilibrium prevails between the continuous and the discontinuous fuel phases.

For low values of L_M^* the eflect of the capillary dispersion is to enhance the fuel imbibition leaving more fuel in the discontinuous phase until the equilibrium state is reached at later times.

Acknowledgements—This research was in part supported by a grant from the National Council for Research and Development, Israel, and KFK, Karlsruhe, Germany. M.S. was supported by the Technion V.P.R. Fund-E. Schaver Research Fund and the Bat-Sheva de Rothschild Foundation for the Advancement of Science and Technology.

REFERENCES

ADLER, P. M. & BRENNER, H. 1988 Multiphase flow in porous media. *A. Rev. Fluid Mech.* **20,** 35–59.

BARENBLATT, G. I. 1979 *Similarity, Self-similarity and Intermediate Asymptotics.* Consultants Bureau, New York.

BEAR, J. 1972 *Dynamics of Fluids in Porous Media.* Elsevier, New York.

CHEN, J. D. 1986 Some mechanisms of immiscible fluid displacement in small networks. *J. Colloid Interface Sci.* **110,** 488–503.

HOUGEN, O. A. & MARSHAL, W. R. 1947 Adsorption from fluid stream flowing through a stationary granular bed. *Chem. Engng Prog.* **43,** 197–208.

LAND, C. S. 1968 Calculation of imbibition relative permeability for two and three-phase flow from rock properties. *Soc. Pet. Engrs J.* **8,** 149–156.

LAND, C. S. 1971 Comparison of calculated with experimental imbibition relative permeability. *Soc. Pet. Engrs J.* **23,** 419–425.

LEVINE, S., LOWNDE, J. & REED, P. 1980 Two-phase fluid flow and hysteresis in periodic capillary tube. *J. Colloid Interface Sci.* **77,** 253–263.

MORROW, N. R. 1970 Physics and thermodynamics of capillary action. In *Flow Through Porous Media* (Edited by NUNGE, R. J.), pp. 102–128. American Chemical Society, Washington, D.C.

MORROW, N. R. & HARRIS, C. C. 1965 Capillary equilibrium in porous materials. *Soc. Pet. Engrs J.* **5,** 15–24.

PAYATAKES, A. C. 1982 Dynamic of oil ganglia during immiscible displacement in water wet porous media. *A. Rev. Fluid Mech.* **14,** 365–393.

PFANKUCH, H. O. 1984 Determination of the contaminant source strength from mass exchange processes at petroleum ground water interface in shallow aquifer systems. In *Proc. Petroleum Hydrocarbons and Organic Chemical in Groundwater—Prevention Detection and Restoration*; *National Water Well Assoc. Conf.*, Houston, Tex.

PISTINER, A., SHAPIRO, M., & RUBIN, H. 1989a Fuel pollutant migration in porous media: analysis of free boundaries. *Transp. porous Media.* Submitted.

PISTINER, A., RUBIN, H. & SHAPIRO, M. 1989b Migration of an immiscible contaminant in a water flow through a double porosity porous medium. *Israel J. Technol.* Accepted for publication.

RAMAKRISHNAN, T. S. & WASAN, D. T. 1986 Effect of capillary number on the relative permeability function for two-phase flow in porous media. *Powder Technol.* **48,** 99–124.

RAMAKRISHNAN, T. S., WILKINSON, D. & DIAS, M. 1988 Effect of capillary pressure on the approach to residual saturation. *Transp. porous Media* **3,** 51–79.

ROSENFELD, J. I. & WASAN, D. T. 1974 Coalescence of drops in liquid–liquid dispersion through a fibrous bed. *Can. J. chem. Engrs* **52,** 3–9.

SLATTERY, J. C. 1979 Interfacial effects in the displacement of residual oil by foam. *AIChE Jl* **25,** 283–289.

SOO, H. & RADKE, C. J. 1986 Filtration model for the flow of dilute stable emulsions in porous media. *Chem. Engng Sci.* **41,** 263–272.

SPIELMAN, L. A. 1977 Particle capture from low-speed laminar flows. *A. Rev. Fluid Mech.* **9,** 297–319.

SPIELMAN, L. A. & GOREN, S. L. 1972 Theory of coalescence by flow through porous media. *Ind. Engng Chem. Fundam.* **1,** 66–73.

SPIELMAN, L. A. & SU, Y. P. 1977 Coalescence of oil in water suspensions by flow through porous media. *Ind. Engng Chem. Fundam.* **16,** 272–282.

TONDEUR, D. 1987 Unifying concepts in non-linear unsteady processes Part I: solitary travelling waves. *Chem. Engng Process.* **21,** 167–178.

WILSON, J. L. & CONRAD, S. H. 1984 Is physical displacement of residual hydrocarbons a realistic possibility in aquifer restoration? In *Proc. Petroleum Hydrocarbons and Organic Chemicals in Groundwater—Prevention Detection and Restoration*; *National Water Well Assoc. Conf.*, Houston, Tex.

YORTSOS, U. C. & FOKAS, A. S. 1983 An analytical solution for linear waterflood including the effects of capillary pressure. *Soc. Pet. Engrs J.* **23,** 115–124.